STOCHASTIC GRAIN BOUNDARY FAILURE AND GEOMETRICAL MODELS OF CREEP DAMAGE

H. Riesch-Oppermann[1] , A. Brückner-Foit[2]

A geometrical model for the grain structure of a polycrystalline material forms the basis of a statistical model of creep damage. Damage is introduced into the grain boundary structure by failure of the grain boundary facets. Microscopic damage is related to the macroscopic behaviour of the material by use of suitable relations such as creep potentials which relate damage parameters on a microscopic level to macroscopic quantities such as the creep strain rate and the creep life. Two examples with different materials are presented together with experimental and simulation results.

INTRODUCTION

The paper intends to show how the scatter of the macroscopic creep damage can be related to the scatter of the microstructure of the material, which is an important task in the field of lifetime predictions based on micromechanical models of creep damage. The basic idea is to perform statistical simulations of creep damage on a microscopic level and to have then a parameter, which allows to relate the microscopic damage to macroscopic quantities like the creep strain rate or the creep life. This parameter should also be related to experimental investigations of creep damage.

In the following, a specific class of creep damage is considered. Damage is assumed to be caused by the nucleation and growth of voids on grain boundaries. In this case, the scatter in the microstructural area comes mainly from two sources. The first is the geometrical one, characterized by the scatter in grain size and orientation of the grain boundaries. The second source is damage-related and is characterized by the scatter of the input-variables for local damage evolution.

This leads to a simulation procedure consisting of two steps: In a first step, the grain boundary structure of the material, as it appears in metallographic sections, is simulated. In a second step, damage is introduced into the grain boundary structure. The results of the simulation have then to be compared with experimental results in order to draw conclusions about the applicability of the selected models. Modifications and improvements of the models have to be

1 Kernforschungszentrum Karlsruhe, Institut für Materialforschung II, P.O. Box 3640, D-76021 Karlsruhe, FRG

2 Universität Karlsruhe, Institut für Zuverlässigkeit und Schadenskunde im Maschinenbau, P.O. Box 3640, D-76021 Karlsruhe, FRG

made according to experiments. It is shown how the simulation of the microstructure can be performed using methods of stochastic geometry, how the simulated microscopic damage can be incorporated in a macroscopic formulation and how simulated and experimental results fit together.

CREEP DAMAGE BY CAVITATING GRAIN BOUNDARY FACETS

On a micromechanical scale, different mechanisms of creep damage can be identified [1]. An important creep damage mechanism is the formation and growth of voids on grain boundaries. In metals, voids nucleate mainly on grain boundaries which are oriented perpendicularly to the loading direction. Existing voids grow by stress directed diffusion of matter from the surface of the void into the grain boundary. The growth rate of the voids is proportional to the normal stress σ_b acting on the grain boundary.

Two limiting cases of void growth can be distinguished. If the stress σ_b acting on the grain boundary coincides with the remote applied stress σ_n, void growth is stress-controlled. This corresponds to a situation where we have 'isotropic damage' of the material with the amount of cavitation on each grain boundary being representative for the whole section of the material. For isolated cavitating facets, however, the surrounding grains, which have non-cavitated grain boundaries, may have a supporting influence on the cavitated grain boundary, which leads to a relaxation of the normal stress σ_b that controls void growth. If the stress on the grain boundary relaxes completely ($\sigma_b \simeq 0$) the cavitated facet acts as a microcrack [2]. The growth of voids is then mainly determined by the deformation of the adjacent grains and becomes thus strain-controlled. $\sigma_b \simeq 0$ corresponds to a situation where the nucleation of voids on the grain boundary is identical with the formation of a microcrack. In an advanced stage of damage, the isolated microcracks begin to interact and coalesce. Final failure occurs by formation of a dominating crack.

This damage mode, which has been observed in creep experiments, will be considered in this paper.

RELATION BETWEEN MICROSCOPIC DAMAGE AND MACROSCOPIC RESPONSE

The presence of microcracks in a material affects its macroscopic deformation behaviour. Hutchinson [3] gives an expression for the creep strain rate of a material containing sparsely distributed (i.e. non-interacting) penny-shaped microcracks oriented perpendicularly to the loading direction. The additional deformation rate induced by the presence of microcracks is obtained in terms of a creep potential Φ which consists of a term Φ_0 related to the undamaged material and a term Φ_c indicating the presence of the microcracks: $\Phi = \Phi_0 + N\ \Phi_c$, where N is the number of cracks per unit volume. The following expression for the creep strain rate is obtained for uniaxial loading and a material obeying NORTON's creep law with parameters B and n: $\dot{\varepsilon} = (1 + \rho)B\sigma^n$, where ρ denotes the damage-induced part of the creep strain rate and is related to the volume density of microcracks, N, by

$$\rho = 0.5\ d^3\ N\ (n+1)\ /\ \sqrt{1+3/n} \qquad \text{for cracks with diameter } d\ .$$

If the interaction of microcracks cannot be neglected, a self-consistent model e.g. as introduced by Riedel [4] leads to the following relationship for the creep strain rate:

$$\dot{\varepsilon} = B\sigma^n\ /\ (1-\rho)\ .$$

The parameter ρ, which plays the role of a damage parameter is related to experimental damage parameters, which can be determined by ultrasonic measurements or from metallographic sections of crept specimens [5].
The important feature of the damage parameter ρ is the fact that it links the microscopic damage and macroscopic creep behaviour of the material and that it is related to experimental damage parameters.

SIMULATION PROCEDURE FOR GRAIN BOUNDARY STRUCTURE AND CREEP DAMAGE

For a given physical model, simulation can replace some part of the experimental investigations by calculations and may lead to the verification of the model under consideration. Using different physical models, simulation can give hints about how these models affect the results. Thus, it is possible to study the influence of specific variables which in turn may lead to deeper insight about the dominant mechanisms.
In our case, the simulation procedure consists of two steps: In a first step, the grain boundary structure as it appears in metallographic sections is simulated. In a second step, damage is introduced into the grain boundary structure.
If we assume that grains form by isotropic crystallization starting from germs in a metallic melt, grain boundaries of neighbouring grains are the midplanes of the respective germs. Mathematically, the germs are created as outcomes of a Poisson-point-process in a certain part of the plane which is called window for convenience. Each point is associated with a cell consisting of all points whose distance to the respective point is less than to all other points of the window. This leads to a partition of the window into cells, the so-called Dirichlet tesselation (also known as POISSON-VORONOI-mosaic). The cells of the Dirichlet tesselation correspond to the grains of a metallographic section and the boundaries of the cells to the grain boundaries.
Here we idealize in the sense that we assume the locations of the germs to be in the plane of the metallographic section, which is not true but seems to be a reasonable assumption for the time being.
The Dirichlet tesselation is determined by use of an algorithm given by Green & Sibson [6]. The great advantage of this algorithm is that it allows to include additional points into a given configuration, with the amount of work necessary for this being almost independent of the number of existing grains. Upon completion of the algorithm, we have for each grain a so-called contiguity list of adjacent grains and the coordinates of the grain boundaries which in a later

stage can be used to model interaction effects of neighbouring grain boundaries which is normally a very complicated and time-consuming task.
The first step of the simulation is now completed. A random grain boundary structure is obtained which is based on randomly distributed germs in a window which can be thought of as part of a metallographic section. The characteristics of this grain boundary pattern depend on the characteristics of the underlying point process. Now, in a second step, damage has to be introduced into the grain boundary structure. A criterion for the failure of a grain boundary facet is necessary to model creep damage by formation of microcracks on a grain boundary. At the moment, this is not yet available. Damage is therefore modeled in a qualitative way. Experimental investigations of an austenitic steel show that the formation of microcracks occurs preferentially on grain boundaries which are oriented perpendicularly to the loading direction [5]. This fact is used for the damage simulation of the grain boundary facets.
A failure probability which depends on the orientation of the facet relative to the loading direction is assigned to each facet. The dependencies of grain boundary failure on other parameters is included in the failure probability in terms of a reference value for the failure probability. This corresponds to the assignment of a certain 'damage level'. At the end of the simulation procedure, a list of cavitated and non-cavitated boundaries for each grain of the random cell structure is obtained.

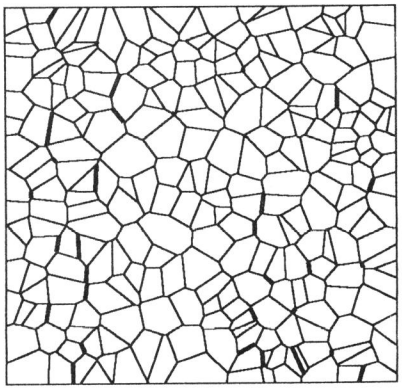

Figure 1. Simulated metallographic section by use of Dirichlet tesselation

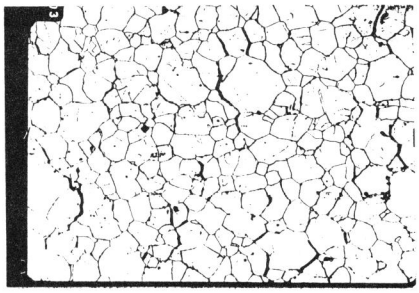

Figure 2. Metallographic section of the austenitic steel AMCR 0033

COMPARISON BETWEEN SIMULATION AND EXPERIMENT

For the time being, damage is introduced into the simulated grain boundary configuration in a purely phenomenological way. Naturally, one can only expect a qualitative result from this approach. Figure 1 and Figure 2 show damage patterns obtained by simulation and from experiments, respectively. The metallographic section was obtained within investigations of creep damage of an austenitic steel AMCR 0033, which were performed at the JRC Ispra [5]. This kind of material shows damage by failure of grain boundary facets, which are

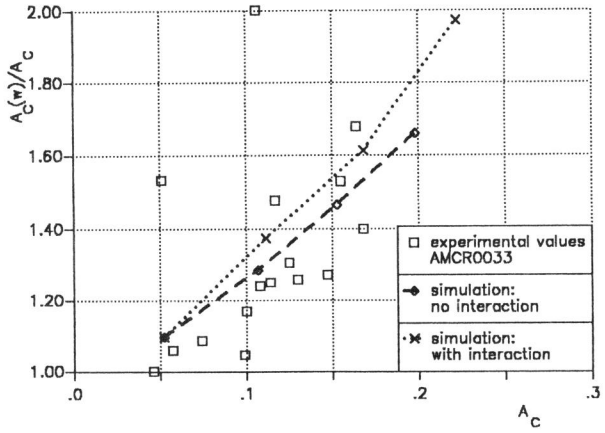

Figure 3. Assessment of interaction effects

oriented perpendicularly to the loading direction. For the simulation of damage, no specific damage mechanism of the grain boundary facets is included. It is merely assumed that damage of the grain boundaries depends on the orientation with respect to the loading direction. Nevertheless, at a first glance, simulated and experimentally obtained damage patterns show a surprisingly good agreement.

Obviously, more quantitative measures are needed to characterize the differences and the common features of simulated and experimental patterns. Experimentally, damage is determined by line section methods which lead to an estimation of a damage parameter A_c, the fraction of cavitated grain boundaries along a test line on the surface of the metallographic section. The simulated patterns can be evaluated in the same way with the advantage that bias resulting from different treatments of simulated and experimental results can be avoided.

To assess damage interaction effects, that is, effects of the presence of an existing microcrack on the failure of adjacent grain boundary facets, a weighted form of the parameter A_c can be used. The weighted form $A_c(w)$ of the damage parameter A_c is obtained by counting a cavitated grain boundary n-fold, if the facet contributes to a microcrack which is made up of n facets [7]. The fraction $A_c(w)/A_c$, which gives the mean number of facets per crack, can then be plotted against A_c, which is done in Figure 3. Here, damage interaction is modelled by attributing an increased value for the failure probability to grain boundary facets adjacent to existing microcracks, dependent on the number of facets of the already existing microcrack. Figure 3 shows an increase of $A_c(w)/A_c$, which may be due to two reasons: first, there is a purely random effect for the cavitation of facets adjacent to existing microcracks, and second, the increase of $A_c(w)/A_c$ may be due to interaction effects. As can be seen, the scatter coming from the experimental results is quite large, so that it is not possible to draw any conclu-

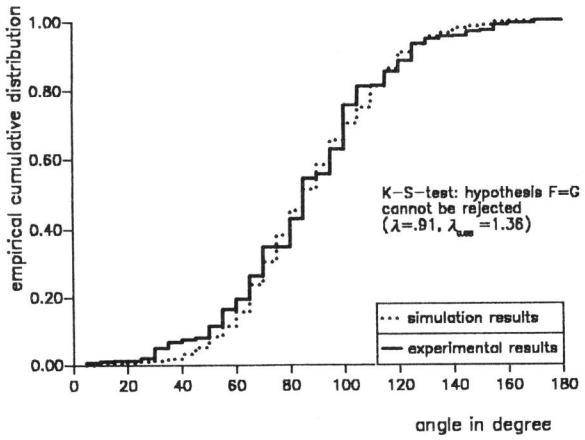

Figure 4. Empirical distribution of crack orientation with loading direction

sions about interaction effects, but the qualitative agreement of experiment and simulation in the tendency of damage evolution is quite surprising.

Quantitative comparisons of simulated and experimentally obtained damage patterns may also be obtained with the help of empirical distributions of some selected quantities. First, the orientation of the cracks which initiate on the grain boundaries is considered. Figure 4 shows the empirical distribution function of the angle between a crack and the loading direction for both simulation and experiment. A statistical Kolmogorov-Smirnov-test shows the distributions of experimental and simulated crack orientations are compatible with each other and, hence, the model chosen for the orientation dependence is in agreement with the findings of the experiment.

Geometrical quantities of the simulated and experimental patterns are also the area of the grains and the length of the formed cracks. These quantities reflect the geometrical differences of the real grain structure and the POISSON-VORONOI-mosaic which is used as geometrical model for the simulation. As there is no natural length scale in the simulation, the median of the grain area distribution is used to adapt the scale of the metallographic section obtained in the experiments and the POISSON-VORONOI-mosaic obtained in the simulation procedure. If we do this, Figure 5 shows that the simulation (DZ1P1000) tends to contain fewer grains with very small grain sizes and also fewer grains with relatively large grain sizes, which means that the distribution of simulated grain areas has smaller variance than that of the experimental grain areas (AMCR0033). This may be due to the fact that we simulate a 2-D mosaic, whereas the metallographic section is a section of a 3-D grain arrangement.

Figure 6 shows the empirical distribution function of the observed together with the simulated crack length. Here, we observe that the simulated crack length tends to be shorter than the experimentally observed one. Two reasons may explain this behaviour. The first reason may be the fact that very short cracks

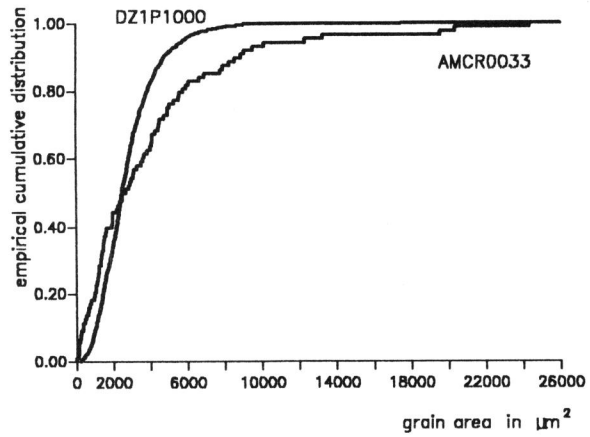

Figure 5. Empirical distribution of grain area. The length scale of the simulation is obtained by imposing identical values of the median for both, experimental and simulated grain structures.

are difficult to find on metallographic sections so that there is a bias in the empirical distribution of the observed crack length. The second reason comes from a specific property of the used 2-D mosaic for the simulation, which has a relatively large fraction of very short edges leading to very short cracks. The first reason leads to a shift of the experimental distribution towards larger crack

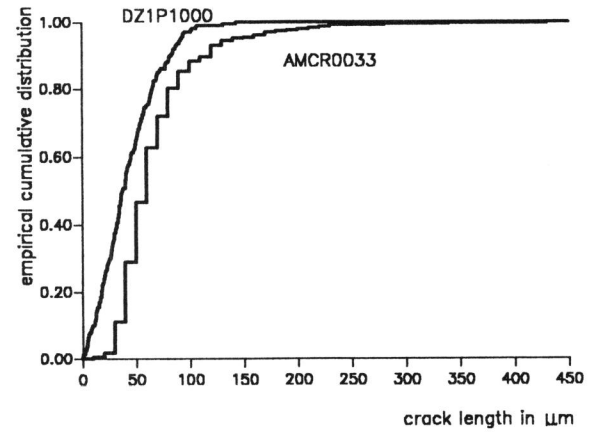

Figure 6. Empirical distribution of crack length

lengths, whereas the second reason leads to a shift of the simulated distribution function towards smaller crack length values.
Hence, while there are inherent differences in the geometrical properties of simulated and experimentally obtained grain structures, the orientation dependence of the underlying damage mechanism is well represented by the simulation model.

CREEP DAMAGE OF CERAMICS: A TENTATIVE EXAMPLE

In the preceding part of the paper, damage introduced into the stochastic grain boundary structure was based on phenomenological arguments rather than on a micromechanical model. In the following, an example will be given where a micromechanical description of damage is used. The purpose of this example is to show that identical grain boundary configurations may lead to completely different damage patterns depending on the active mechanisms of damage.
The material under consideration is alumina subjected to compressive creep loading. Following Chan & Page [8], nucleation of cavities on grain boundaries occurs as the result of stress concentrations at grain boundary ledges due to discontinuous grain boundary sliding events. The nucleation of cavities is described by classical nucleation theory (see e.g. [4]). The stress concentrations which are necessary to form critical clusters of vacancies on the grain boundary result from two competitive processes: the evolution of stress concentrations when grain boundary sliding occurs by transformation of shear stresses along the grain boundaries into normal stresses on the grain boundary ledges and the relaxation of stress concentrations by grain boundary diffusion. Grain boundary sliding relaxes within a characteristic time, t_{BR}, whereas diffusion processes relax within a characteristic time, t_c. t_{BR} and t_c depend on grain boundary characteristics and diffusion parameters [8]. A time-dependent stress concentration factor q is given by Chan & Page [8] which depends on the characteristic times for grain boundary sliding, t_{BR}, and diffusion, t_c, with

$$q(t) = \frac{1}{2}\left\{\frac{\lambda}{h}\left[1 - \exp(-t/t_{BR})\right]\exp(-t/t_c) + c\right\}$$

where c depends on the kind of loading and on the orientation of the grain boundary, t is time and h, λ are height and spacing of the grain boundary ledges, which are assumed to be periodically distributed along the grain boundary. Nucleation of voids on a grain boundary is assumed to occur if the nucleation rate for the maximum of q, which occurs at time $t = t_{BR} \times \ln(1 - t_c/t_{BR})$, exceeds a certain critical value, which is arbitrarily set to 1. Since nucleation increases very rapidly with the stress level the absolute value of the critical nucleation rate does not affect the results of the simulation qualitatively. The quantities for diffusion and grain boundary structure are treated as deterministic variables and the only source of scatter is the random orientation of the grain boundaries. It is assumed that cavitation occurs in a constrained way, which means that the nucleation of voids on a grain boundary leads to failure of the grain boundary.
Figure 7 shows typical examples of the damage patters obtained for different stress levels. For low stress levels, failed grain boundary facets are oriented pre-

ferentially around an angle of 45° with respect to the loading direction, corresponding to the maximum shear stress, which is responsible for grain boundary sliding. With increasing stress, facets with orientations deviating significantly from 45°, begin to cavitate. These simulations were performed without any experimental background. The aim was to show the flexibility of the stochastic model. From Figure 7 it can be seen that, with the same underlying type of grain boundary structure as in Figure 1, very different damage patterns result as a consequence of the different damage mechanisms.
Experimental observations on creep and grain boundary sliding measurements, however [9], have recently shown that there is no correlation between the amount of grain boundary sliding and the orientation of a grain boundary facet with respect to the loading direction. This could be proved by a statistical test of grain boundary sliding measurement data [10]. We found no significant correlation between grain boundary orientation and the amount of sliding of the grain boundary. Obviously, stress redistribution due to grain boundary sliding leads to unpredictable stresses on the grain boundaries. The statistical model thus has to be updated to account for this, which was not yet done.

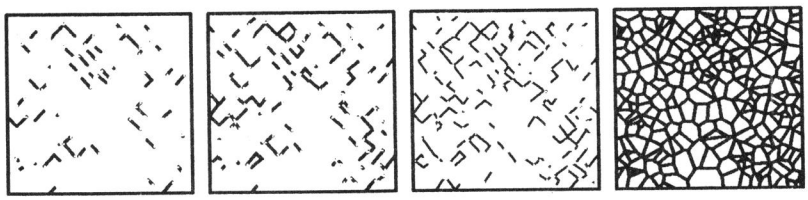

Figure 7. Simulated damage patterns for alumina under compressive creep. Left to right: increasing stress level and complete grain boundary structure

CONCLUSIONS

In this paper, some ideas concerning the statistical modelling of damage on a microstructural level and its relation to macroscopic quantities are given.
Two examples using different kinds of approaches for the damage modelling are presented. In the first example, creep damage of an austenitic steel is modelled in a phenomenological way according to experimental observations. This leads to patterns of simulated grain boundary failure, which are in qualitative agreement with experimental findings. A method is indicated how to incorporate micromechanical models in macroscopic relations for creep behaviour. Some qualitative aspects of the experimentally obtained and the simulated damage patterns are shown.
In the second example, a micromechanical model for creep damage of alumina is incorporated into the simulated grain boundary structure.
Characteristic patterns of the different simulation procedures are shown and illustrate the flexibility of the geometrical model which allows to incorporate any kind of grain boundary failure.
As a first step, the results seem to be encouraging. The advantages of the use of stochastic geometry methods in the light of the possible inclusion of more

sophisticated models for grain boundary failure and the interaction effects of cavitated grain boundary facets are twofold: (1) Any kind of grain boundary failure can be handled by the stochastic model which is therefore applicable to various kinds of material. (2) Interaction effects of cavitated grain boundary facets can be handled in a very efficient way, which allows the simulation of realistic configurations without a prohibitively large amount of computing time.

Acknowledgement: The financial support of the Deutsche Forschungsgemeinschaft under grant No. Mu 466/15-2 is gratefully acknowledged.

REFERENCES

[1] M.F. Ashby, B.F. Dyson, Advances in Fracture Research (Fracture 84), Vol. 1, 3-30.
[2] B.F. Dyson, Scripta Metall. 17 (1983), 31-37.
[3] J.W. Hutchinson, Acta Metall. 31 (1983), 1079-1088.
[4] H. Riedel, Fracture at High Temperatures, Springer, Berlin 1987.
[5] H. Stamm, U. von Estorff, The Use of Creep Damage Measurements in Combination With Material Models for Residual Lifetime Assessment, in: ECF 8 Fracture Behaviour and Design of Materials and Structures, Vol.3, Torino, 1990, 1202-1208.
[6] P.J. Green, R. Sibson, The Computer Journal 21 (1978), 168-173.
[7] H. Riedel, Int. J. Pres. Ves. & Piping **39** (1989), 119-134
[8] K.S. Chan, R.A. Page, J. Mat. Sci. 25 (1990), 4622-4629.
[9] C.R. Blanchard, R.A. Page, J. Am. Ceram. Soc. 75 (1992), 1612-1620.
[10] C.R. Blanchard, Personal Communication.